



ELSEVIER

Available online at www.sciencedirect.com

SCIENCE @ DIRECT®

Journal of volcanology
and geothermal research

Journal of Volcanology and Geothermal Research 129 (2004) 237–259

www.elsevier.com/locate/jvolgeores

Internal structure of Puna Ridge: evolution of the submarine East Rift Zone of Kilauea Volcano, Hawai'i

Stephen C. Leslie^{a,1}, Gregory F. Moore^{a,*}, Julia K. Morgan^b

^a Department of Geology and Geophysics, University of Hawai'i, Honolulu, HI 96822, USA

^b Department of Geology and Geophysics, Rice University, Houston, TX 77005, USA

Received 31 July 2002; accepted 3 July 2003

Abstract

Multichannel seismic reflection, sonobuoy, gravity and magnetics data collected over the submarine length of the 75 km long Puna Ridge, Hawai'i, resolve the internal structure of the active rift zone. Laterally continuous reflections are imaged deep beneath the axis of the East Rift Zone (ERZ) of Kilauea Volcano. We interpret these reflections as a layer of abyssal sediments lying beneath the volcanic edifice of Kilauea. Early arrival times or 'pull-up' of sediment reflections on time sections imply a region of high P-wave velocity (V_p) along the submarine ERZ. Refraction measurements along the axis of the ridge yield V_p values of 2.7–4.85 km/s within the upper 1 km of the volcanic pile and 6.5–7 km/s deeper within the edifice. Few coherent reflections are observed on seismic reflection sections within the high-velocity area, suggesting steeply dipping dikes and/or chaotic and fractured volcanic materials. Southeastward dipping reflections beneath the NW flank of Puna Ridge are interpreted as the buried flank of the older Hilo Ridge, indicating that these two ridges overlap at depth. Gravity measurements define a high-density anomaly coincident with the high-velocity region and support the existence of a complex of intrusive dikes associated with the ERZ. Gravity modeling shows that the intrusive core of the ERZ is offset to the southeast of the topographic axis of the rift zone, and that the surface of the core dips more steeply to the northwest than to the southeast, suggesting that the dike complex has been progressively displaced to the southeast by subsequent intrusions. The gravity signature of the dike complex decreases in width down-rift, and is absent in the distal portion of the rift zone. Based on these observations, and analysis of Puna Ridge bathymetry, we define three morphological and structural regimes of the submarine ERZ, that correlate to down-rift changes in rift zone dynamics and partitioning of intrusive materials. We propose that these correspond to evolutionary stages of developing rift zones, which may partially control volcano growth, mobility, and stability, and may be observable at many other oceanic volcanoes.

© 2004 Elsevier B.V. All rights reserved.

Keywords: Hawai'i; Kilauea Volcano; rift zone; dike complex; seismic reflection; gravity

1. Introduction

Volcanic rift zones are primary structural components of oceanic island volcanoes, and have been described in many settings, for example, the islands of Hawai'i, the Canaries, and sub-

¹ Present address: ChevronTexaco Exploration and Production Technology Company, San Ramon, CA 94583, USA.

* Corresponding author. Tel.: +1-808-956-6854;
Fax: +1-808-956-5154.

E-mail address: gmoore@hawaii.edu (G.F. Moore).

merged guyots throughout the Pacific Basin (e.g., Fiske and Jackson, 1972; Vogt and Smoot, 1984; Gee et al., 2001). These features are thought to play important roles in volcanic structure and evolution. Volcanoes grow largely by surface eruptions localized along the rift axes, fed by subsurface dikes that propagate parallel to the rift at depth (Moore and Krivoy, 1964; Fiske and Jackson, 1972; Dieterich, 1988). Through time, rift zones can evolve into extensive, elongate ridges that transport magma far from the volcano summit. The dynamics of dike propagation that feeds intrusion and eruption has been the subject of numerous studies, which demonstrate the interplay among such factors as magma flux, pressure gradient, dike width, topographic slope, and regional stress field (e.g., Fiske and Jackson, 1972; Dieterich, 1988; Fialko and Rubin, 1999; Parfitt et al., 2002). Shallow dikes within the rift are also underlain by stratified complexes of intrusive rocks, including dense cumulates (e.g., Hill and Zucca, 1987; Okubo et al., 1997; Kauahikaua et al., 2000), which may play a role in destabilizing the volcano flanks (Clague and Denlinger, 1994). Discrete volcanic sectors undergo relative displacement, and are capable of catastrophic collapse (e.g., Swanson et al., 1976; Denlinger and Okubo, 1995; Moore and Krivoy, 1964; Moore et al., 1989; Iverson, 1995). Ultimately, the persistence of distinct volcanic rift zones may determine the rate of growth and lifespan of active volcanoes (e.g., Fiske and Jackson, 1972; Dieterich, 1988).

Despite high-quality topographic, bathymetric, geological, and geophysical data over oceanic volcanic rift zones (e.g., Fornari, 1987; Lonsdale, 1989; Clague et al., 1994; Gee et al., 2001), comparatively little is known about the processes by which rift zones initiate and develop. Along the best studied on-land portions, the earliest stages of rift zone evolution are commonly overprinted and masked by subsequent volcanic activity. Active rift zones that still exhibit early growth stages are few; the best known example is the East Rift Zone (ERZ) of Kilauea Volcano, Hawai'i. The ERZ stretches nearly 125 km from the SE edge of Kilauea's summit, into the axis of the sur-

rounding Hawaiian Deep (Fig. 1). The ~75 km long submarine extension, known as Puna Ridge, defines a tapering prism of volcanic material, up to ~5000 m high, that laps down onto the abyssal seafloor at its distal end (Fig. 1). Rift zone activity and ridge morphology vary along the length of the ERZ (e.g., Fornari et al., 1978; Lonsdale, 1989; Clague et al., 1994; Smith et al., 2002a; Parfitt et al., 2002). The ERZ of Kilauea, therefore, provides a rare opportunity to examine the evolving structure of an active rift zone, and to correlate these observations with volcanic processes along its length.

The comparatively mature subaerial ERZ has been the subject of decades of geologic mapping; monitoring of eruptive activity, ground motions, and seismicity; and geophysical surveying (e.g., Kinoshita et al., 1963; Swanson et al., 1976; Broyles et al., 1979; Lipman et al., 1985; Klein et al., 1987; Delaney et al., 1990; Owen et al., 1995; Kauahikaua et al., 2000). From these exercises, models for the internal structure and composition have been developed, and continuously refined. Other than surficial mapping and sampling over Puna Ridge (Fornari et al., 1978; Holcomb et al., 1988; Lonsdale, 1989; Smith et al., 2002a; Johnson et al., 2002), however, few analogous data exist for the submarine rift zone that represents the earliest stages of rift zone growth.

In this paper, we present new multichannel seismic (MCS) reflection, seismic refraction, gravity, and magnetic data collected during a survey conducted in 1998 aboard the R/V *Maurice Ewing* over Puna Ridge and the adjacent Hilo Ridge, which extends offshore from the flank of Mauna Kea (e.g., Holcomb et al., 2000; Smith et al., 2002b). These data demonstrate significant variations in geophysical character and subsurface structure along the length of Puna Ridge, which correlate with spatial changes in ridge morphology and setting. The new data provide support for the phased evolution of volcanic rift zones as they build in size, suggesting fundamental down-rift changes in rift zone dynamics and partitioning of intrusive phases. In turn, these changes may partially control volcanic growth, mobility, and stability.

2. Geologic setting

2.1. Hawaiian rift zones

Along the Hawai'i–Emperor Seamount chain, volcanoes commonly form prominent, elongate rift zones that radiate from their summit regions and extend to abyssal depths (Stearns and Macdonald, 1946; Fiske and Jackson, 1972; Macdonald et al., 1983; Fornari, 1987). Eruptions concentrate along these rift zones, creating long volcanic ridges (in some cases > 100 km) by repeated dike intrusions and flank eruptions (Fiske and Jackson, 1972). Kilauea Volcano, located near the SE end of the Hawai'i–Emperor volcanic chain on the island of Hawai'i (Moore and Clague, 1992), is among the most active and comprehensively studied volcanoes on earth (e.g., Swanson et al., 1976; Tilling and Dvorak, 1993), and is built

upon the SE flank of the larger neighboring volcano Mauna Loa (Fig. 1). Two principal rift zones extend from Kilauea's summit caldera, the highly active, subaerial and submarine ERZ, and the much less active, predominately subaerial Southwest Rift Zone (Moore and Fiske, 1969; Swanson et al., 1976; Wolfe et al., 1987; Lonsdale, 1989). Much of what is known about Hawaiian rift zone structure and processes stems from research at Kilauea Volcano.

The axes of subaerial Hawaiian rift zones are typically marked by strong geophysical anomalies. Gravity surveys over Kilauea's subaerial ERZ show a strong anomaly of ~15 mGal, offset to the northeast of the rift axis (e.g., Kinoshita et al., 1963; Swanson et al., 1976), that appears to continue offshore over Puna Ridge (Kauahikaua et al., 2000). The gravity high correlates with a broad zone of high compressional wave velocities

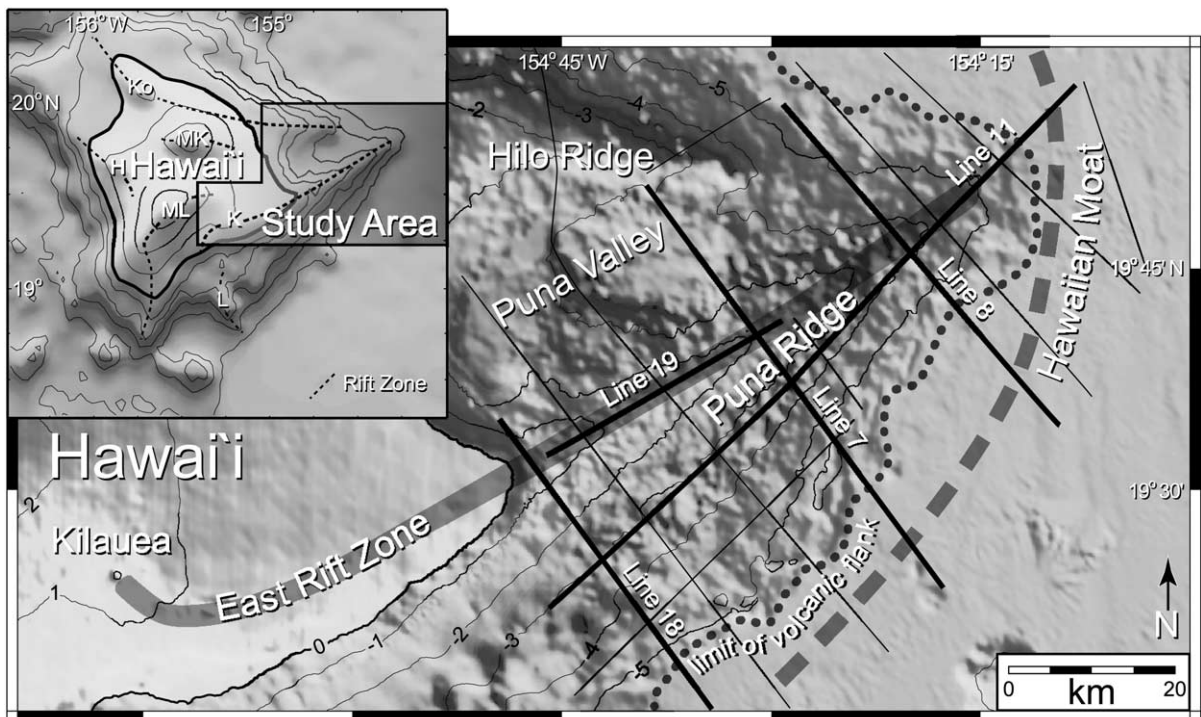


Fig. 1. Location map of survey region. Inset shows the island of Hawai'i with the major volcanoes (Ko-Kohala, H-Hualalai, MK-Mauna Kea, ML-Mauna Loa, K-Kilauea, L-Loihi). Rift zones are marked as dashed lines. Large map shows Kilauea and the orientation of the ERZ (dark shading) and its submarine expression, Puna Ridge. Older Hilo Ridge to the north is separated from Puna Ridge by Puna Valley. Survey lines are shown as thin dark lines; heavy lines show the locations of seismic reflection lines shown in Figs. 4 and 5. Contour interval is 1000 m. Axis of Hawaiian Moat is shown as a heavy dashed line.

(V_p) of 6.5–7.3 km/s beneath the summit and rift zone, contrasting with ~ 3 –5 km/s for the surrounding rocks (Broyles et al., 1979; Hill and Zucca, 1987). This feature is explained by concentrations of high-density, high- V_p dikes that intruded along the cores of the rift zone. Localized seismicity associated with dike intrusion events along the rift zone constrains dike emplacement to within 2–4 km of the surface (Klein et al., 1987; Rubin and Pollard, 1987), defining a triangular prism that widens with depth (e.g., Hill and Zucca, 1987). The width of the intrusive core has been estimated at 12–20 km beneath the subaerial ERZ (Broyles et al., 1979; Furumoto, 1978; Hill and Zucca, 1987). Deep zones of higher-velocity material ($V_p > 7$ km/s) near the base of the volcanic edifice have been interpreted as accumulations of dense olivine cumulates (Hill and Zucca, 1987; Okubo et al., 1997). Interpreted depths for the cumulate materials, based on gravity data, place the cumulates within the oceanic crust at great distances along the rift zones (Kauahikaua et al., 2000), posing the possibility that magmas have intruded vertically through the oceanic crust along the rift zone.

The great intrusive volume implied by the extent of high-density, high-velocity materials beneath Hawaiian rift zones (e.g., Hill and Zucca, 1987; Okubo et al., 1997) must be accommodated by displacements of the volcanic flanks (e.g., Swanson et al., 1976). Ongoing geodetic monitoring demonstrates continuous creeping motion of Kilauea's south flank, up to 10 cm/yr, headed along the upper ERZ (e.g., Owen et al., 1995, 2000; Delaney et al., 1998). Even greater rates of rift extension were documented prior to the onset of present eruptive activity at Pu'u O'o and Kupai'anaha vents along the ERZ (Delaney and Denlinger, 1999). Flank slip is thought to be facilitated by a layer of weak oceanic sediment trapped between the volcanic edifice and the top of the oceanic plate (Ando, 1979; Nakamura, 1980; Crosson and Endo, 1982; Denlinger and Okubo, 1995). This may also be a necessary condition for the creation of persistent, elongate volcanic rift zones (e.g., Fiske and Jackson, 1972; Dieterich, 1988).

The general growth of Hawaiian rift zones, and

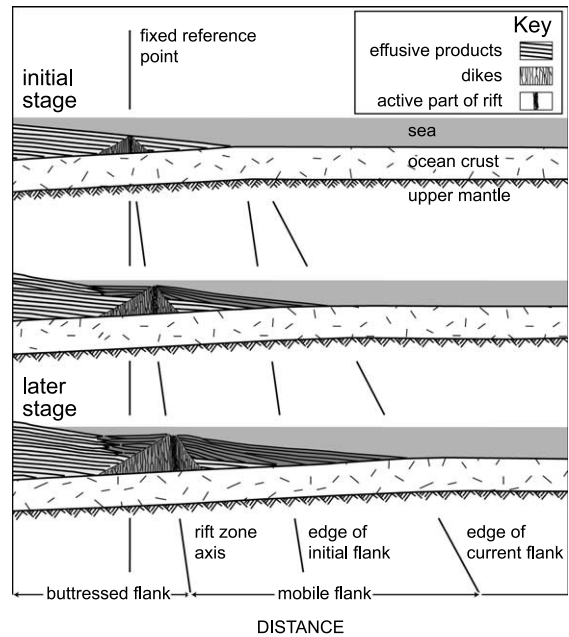


Fig. 2. Schematic cross-sections of the growth of a Hawaiian rift zone on the flanks of an older, still active volcano – from Hill and Zucca (1987). Note the predicted asymmetric profile of the dike complex. As successive dikes intrude into the rift zone and the rift zone grows in height, the seaward, ‘unbuttressed’ side of the volcano slides along the top of the oceanic crust, probably upon a layer of weak, pre-existing sediments.

Kilauea's ERZ built upon pre-existing Mauna Loa flank in particular, is captured by a model proposed by Hill and Zucca (1987). They call for the progressive intrusion of high-density dikes along the rift zone axis, which are subsequently displaced laterally and mantled by lower-density effusive volcanic rocks, as the edifice grows (Fig. 2). Along Kilauea's ERZ, the resulting intrusive core is triangular and asymmetric in cross-section, as new dikes intrude on the seaward side of the dike complex, owing to the buttressing effect of the older edifice of Mauna Loa. Hill and Zucca (1987) note that the deeper structure of the on-land rift zones has been only loosely constrained by the available refraction and gravity data. The offshore regions of the rift zones are even less well understood.

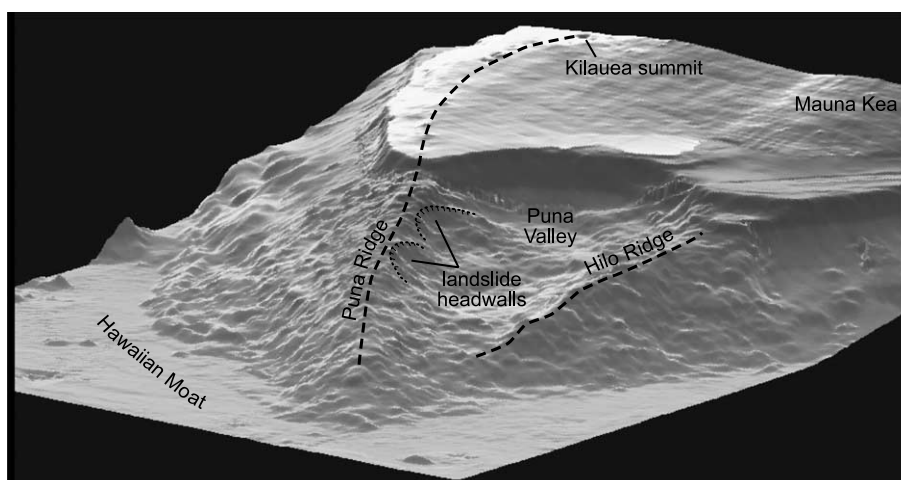


Fig. 3. 3D image of the northeastern portion of the volcanic edifice of Hawai'i (bathymetry from Smith et al., 2002b). Note the arcuate landslide scars (dashed lines) along the northern flank of Puna Ridge facing Puna Valley (Moore and Chadwick, 1995). Dashed line indicates approximate location of Kilauea's ERZ.

2.2. Puna Ridge

The submarine ERZ follows the axis of Puna Ridge, forming a broad, tapering prism that begins at the east cape of the island of Hawai'i and terminates near the axis of the Hawaiian Moat, approximately 5000 m below sea level (Malahoff and McCoy, 1967; Moore, 1971) (Fig. 3). The wealth of data and observations over the subaerial ERZ is not matched for the submarine portion. Studies of Puna Ridge have relied primarily upon surficial observations and samples (e.g., multi-beam bathymetry, side-scan sonar, deep-tow photography, dredge sampling) to infer the deeper structure and processes of formation of the submarine rift zone (Fornari et al., 1978; Holcomb et al., 1988; Lonsdale, 1989; Smith and Cann, 1999; Johnson et al., 2002; Smith et al., 2002a).

The submarine slopes of Puna Ridge vary along its length, and may be indicative of associated volcanic processes. The gradient along the subaerial ERZ from the summit caldera to the coast is very regular at 23 m/km (1.3°). The submarine crest of Puna Ridge also maintains a consistent, but steeper gradient of 50 m/km (3°) to a depth of 2800 m. Below 2800 m, the crest plunges more steeply, at 100 m/km (6°), with several uneven steps in its profile (Lonsdale, 1989). The flanks

of Puna Ridge are steeper than the ridge crest, typically maintaining gradients of 140–210 m/km ($8\text{--}12^\circ$) on transverse profiles (Lonsdale, 1989). Smith and Cann (1999) show that the NW flank slope is highly variable and complex, whereas that of the SE flank does not change significantly until the crest is deeper than 3500 m. They interpret this to indicate that lavas have been added uniformly to the SE flank with time, largely by channeled lava flows in tubes that can transport the lava down slope.

High-resolution multi-beam bathymetric data collected over the length of the ridge reveal extensive lava terraces, circular volcanic vents, and craters covering the surface of the ridge (Clague et al., 1994; MBARI Mapping Team, 2000; Smith et al., 2002a,b). Clague et al. (1994) interpreted large rotational slump blocks along the SE flank of the ridge, responsible for the low terraces near the base of the flank; similarly, Moore and Chadwick (1995) document a steep amphitheater on the north side of the ridge, and speculate that mass wasting of the north flank has contributed avalanche debris to nearby Puna Valley (Fig. 3).

Deep-towed side-scan sonar and photography show the axis of the ridge at depths of 2–4 km to be dominated by numerous gaping fissures, lava flows and collapse pits, interpreted to be the result of repeated intrusive events (Lonsdale,

1989; Smith et al., 2002a). Submersible dives and seafloor photographs reveal pillow lava, lava tubes, lava flow fields, pillow lava ridges, constructional cones, and lava terraces on the crest of Puna Ridge (Fornari et al., 1978; Clague et al., 2000; Smith et al., 2002a). Stepped topography at the tip of Puna Ridge has been interpreted to define a lava apron composed of lava fields separated by scarps 100–200 m high (Lonsdale, 1989). These various studies suggest that the crest of Puna Ridge is the site of numerous dike intrusions and eruptions fed by magma, probably propagating down-rift from the summit area of Kilauea (Lonsdale, 1989; Smith and Cann, 1999; Smith et al., 2002a). Based on these surface observations, however, dike injection from below cannot be ruled out.

Volcanism has not been restricted to the morphologic Puna Ridge in this area. GLORIA side-scan sonar surveys also revealed extensive, voluminous sheet flows within the Hawaiian Moat, surrounding the tip of Puna Ridge (Holcomb et al., 1988). The origin of these flows, interpreted from the lack of sediment cover to be comparatively recent (Holcomb et al., 1988), remains uncertain. If they underlie the growing Puna Ridge, then they may influence the dynamics of the ridge as it grows.

The limited geophysical data previously available over Puna Ridge support the general observations on land, at least near the shoreline. A magnetic survey over Puna Ridge was interpreted to show an 11 km wide ‘composite volcanic plug’ extending the length of the submarine rift zone (Malahoff and McCoy, 1967). This width is consistent with estimates by Broyles et al. (1979) from gravity measurements over the lower subaerial ERZ, suggesting that a dike complex between 12 and 17 km wide resided at depth. More recent three-dimensional gravity modeling of the island of Hawai‘i projected the dense central core of the ERZ well offshore with an ENE trend parallel to Puna Ridge, but its offshore extension remains very poorly constrained (Kauahikaua et al., 2000). The lack of further offshore gravity, magnetics, and seismic surveys has precluded more detailed analysis of the causes of slope and morphologic variations over Puna Ridge, and im-

plications for subsequent evolution of the rift zone.

3. Data acquisition and processing

We collected a grid of 11 seismic reflection profiles and one sonobuoy seismic refraction line over Puna Ridge and nearby areas (Fig. 1) using an airgun array with a volume of 71 l (4336 in³) fired at 50-m intervals. Data were received with a 160-channel, 4.2-km streamer with a group interval of 25 m, yielding 40-fold coverage with 12.5-m common mid-point spacing.

Seismic data processing followed a standardized sequence (Table 1) using ProMAX software at the University of Hawai‘i. Recognition of coherent reflections beneath the volcanic flanks was hindered by the irregular bathymetry of the seafloor that caused scattering of reflected energy and introduced out of plane reflections (see Hills et al., 2002 for more details). In regions of shallow seafloor depth, significant imaging problems were introduced by seafloor multiple reflections. To improve our recognition of reflection events, we performed constant-velocity stacks and viewed the reflection profiles in panels ranging from 1500 to 6000 m/s. Animations of successive velocity panels aided interpretation by clarifying im-

Table 1
Standard processing sequence

Process	Explanation
Edit bad traces	Noisy channels removed from data
Geometry	Shot/receiver definition
Sort to common mid-point (CMP) gathers	12.5-m CMP spacing – 40-fold
Bandpass filter	4-8-72-80 Hz filter
Velocity analysis	Approx. every 100 CMP
Radon filter	Multiple suppression technique
Dip move out (DMO)	Partial migration algorithm
Top mute	Remove noise at far offsets
CMP ensemble stack	
F-K migration	
F-K filter	Remove strongly dipping events
Automatic gain control (AGC)	Scale amplitude of reflections for display

portant reflection events. Some success was attained using radon velocity filtering to suppress seafloor multiples and improve velocity analysis on pre-stack data (Foster and Mosher, 1992; Taylor et al., 1998).

Gravity and magnetic measurements were collected at 1-s intervals during the course of the reflection/refraction survey. On board processing of gravity data included the application of Eötvös corrections and calculation of the free air anomaly. The gravity data were further corrected for submarine terrain effects. For the correction calculation, the submarine edifice was assigned a density of 2600 kg/m³ based upon previous studies (Strange et al., 1965; Watts and ten Brink, 1989; Kauahikaua et al., 2000).

4. Results

4.1. Multichannel seismic reflection data

The MCS survey grid comprises eight transverse and three ridge parallel seismic reflection profiles across Puna Ridge (Fig. 1). Transverse profiles extend from the abyssal Hawaiian Moat, across the southern flank of Puna Ridge to the axis of the submarine ERZ. Reflection profiles 5–9 extend to the northern flank of Puna Ridge and Puna Valley region. In addition, reflection profiles 6 and 7 extend to the northwest and image the adjacent Hilo Ridge. Detailed examination and comparison of successive transverse reflection profiles (Fig. 4) proved especially useful in the structural interpretation of the volcanic edifice. Features on the seismic profiles are keyed below by shot point (SP), two-way travel time, and depth.

The most prominent feature imaged on the reflection profiles is a group of high-amplitude, low-frequency, reverberant reflections that we collectively label horizon A (Fig. 4). These reflections extend from the Hawaiian Moat to directly beneath the axis of Puna Ridge, and occur throughout the survey area (Morgan et al., 2000; Hills et al., 2002; Leslie et al., 2002). Horizon A reflections are evident within ~0.5 s two-way travel time below the seafloor within the Hawaiian

Moat (e.g., Fig. 4, Line 7, SP 200–500), and generally increase in travel time beneath the volcanic edifice, progressively deepening to ~2 s beneath the axis of Puna ridge (Fig. 4, Line 7, SP 900–1000). The continuity of horizon A, its extension into the Hawaiian Moat, and occurrence across the study area indicate that this features lies at or near the top of the pre-existing oceanic crust beneath the volcanic edifice (Morgan et al., 2000; Leslie et al., 2002).

Horizon A forms a broad arch beneath the axis of Puna Ridge on seismic time sections (Fig. 4A,B). This apparent geometry is a distortion effect, caused by the high V_p of the volcanic overburden compared with the surrounding water column (Armstrong et al., 2001). On several of the lines, e.g., Line 7, the axis of this arch is offset ~500 m to the southeast of the topographic axis of the ridge itself (Fig. 4B, inset). This additional distortion is interpreted to result from lateral velocity variations within the volcanic pile. Specifically, a region of high velocity, centered slightly to the southeast of the topographic axis of Puna Ridge, causes additional pull-up of horizon A reflections.

To aid in the structural interpretation of the seismic reflection profiles and high-velocity body, we generated depth sections based upon the assumption that the actual geometry (in depth) of horizon A, parallel to the underlying oceanic crust, is essentially planar and dipping gently towards the volcanic edifice of Hawai'i (e.g., Hill and Zucca, 1987; Thurber and Gripp, 1988; Got et al., 1994). We used a smooth, downward increasing, laterally varying, velocity model for the volcanic edifice, designed to flatten horizon A to the predicted planar geometry (Fig. 4C). Model velocities were fixed at a constant 2.0 km/s at the seafloor, and increased linearly with depth to a maximum of 6.5 km/s directly above the axis of the horizon A arch. Velocity ranges were based upon previous refraction and earthquake location studies of the velocity structure of the volcanic edifice (Hill, 1969; Broyles et al., 1979; Klein, 1981).

The seismic reflection record within the primary volcanic edifice is characterized by less coherent reflections, compared to the laterally continuous

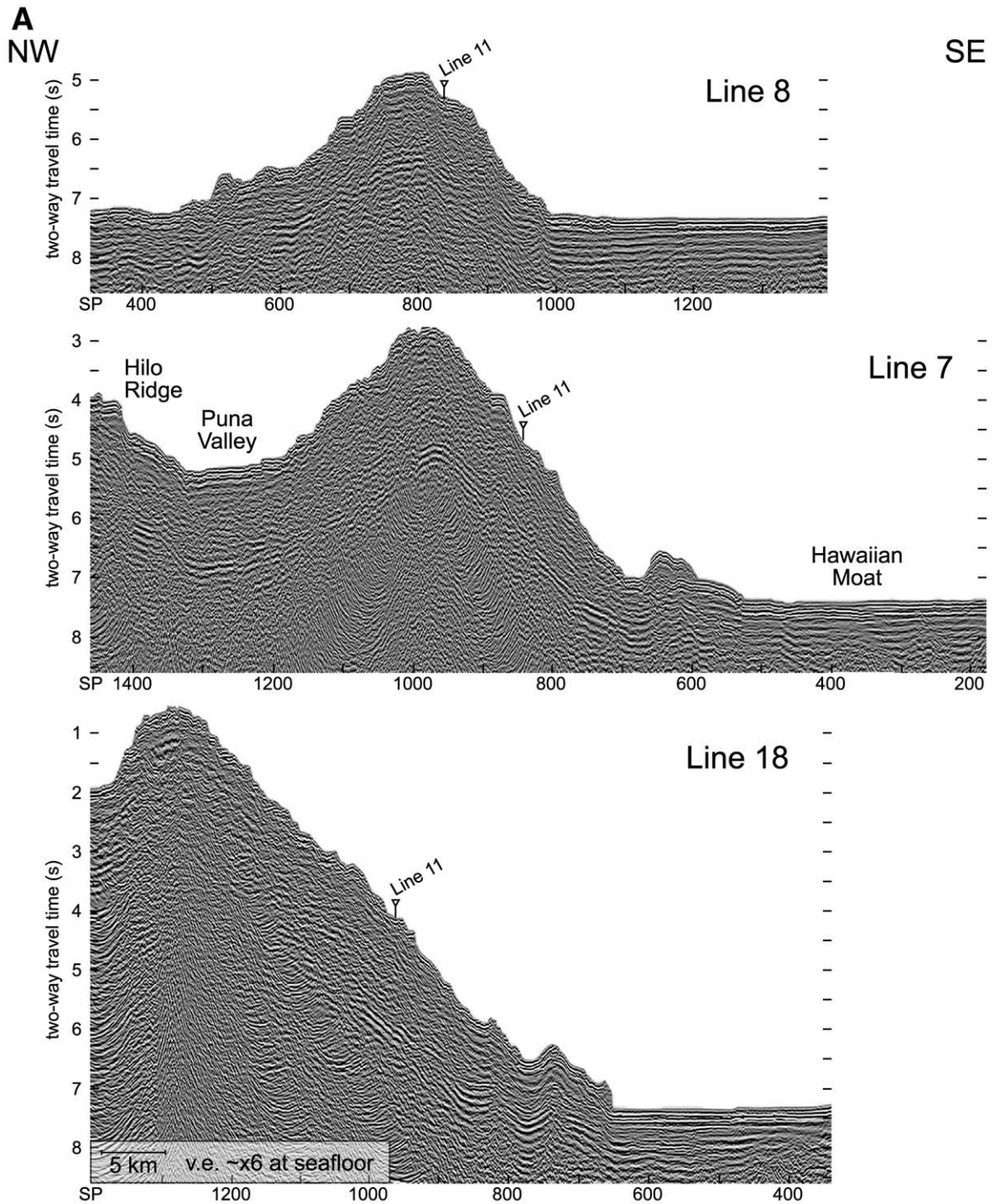


Fig. 4. Transverse seismic reflection profiles across Puna Ridge. Locations of profiles are shown on Fig. 1. SP=shot point number. (A) Uninterpreted time section. Note the continuous reflections that extend from beneath the abyssal seafloor (SE side of lines) to deep within volcanic edifice.

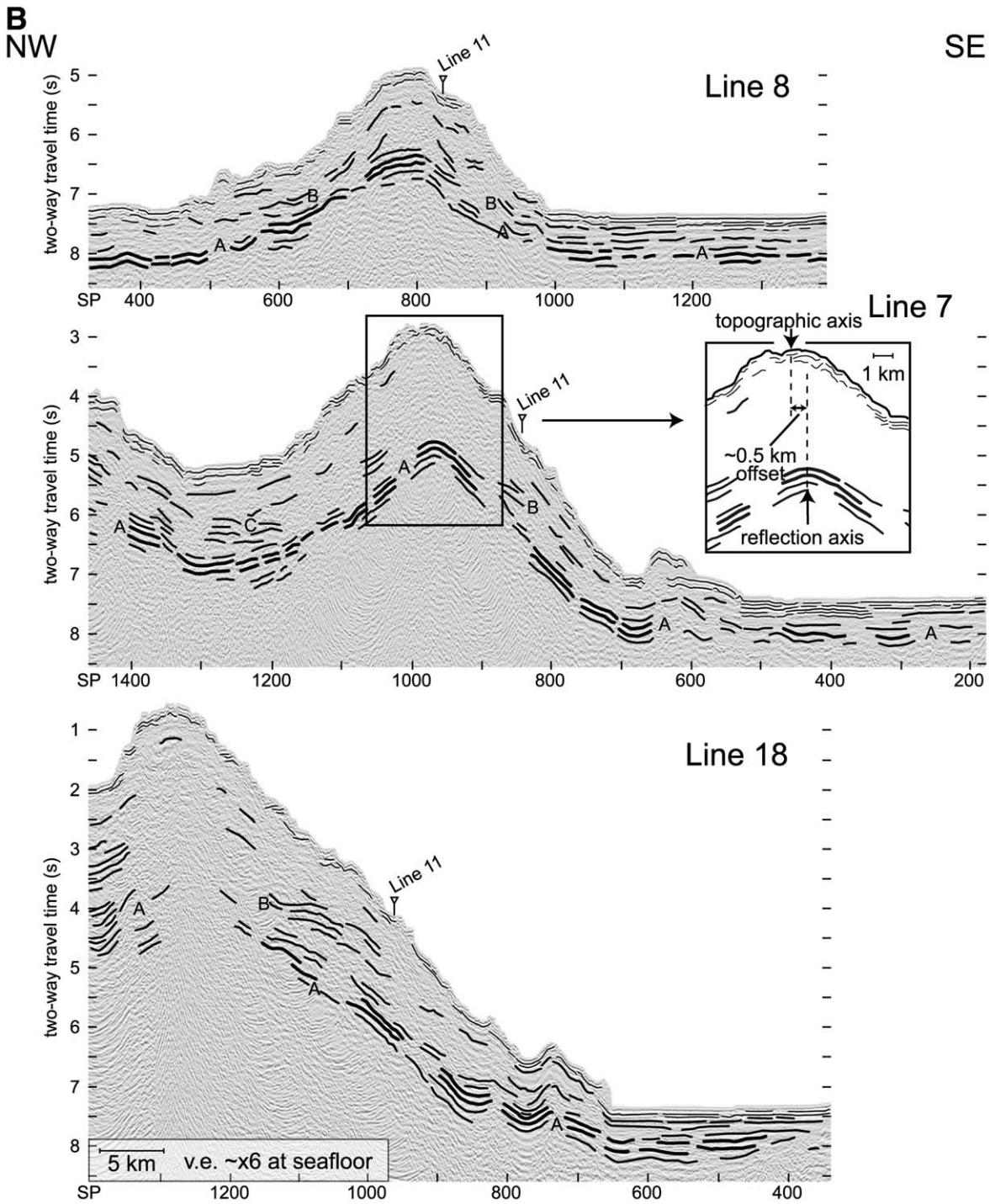


Fig. 4 (Continued). (B) Interpretation of reflection profiles showing horizon A reflections (labeled A). Beneath the SE flank, reflections (labeled B) diverge from horizon A, and guide toward the seafloor. Southeast dipping reflections beneath the NW flank of Puna Ridge (labeled C) may represent the buried flank of Hilo Ridge. Lateral offset of the axis of the ‘pulled-up’ oceanic crust reflection ~ 0.5 km to the southeast of the topographic axis (inset) may be due to variations in the velocity distribution beneath the axis of the ridge.

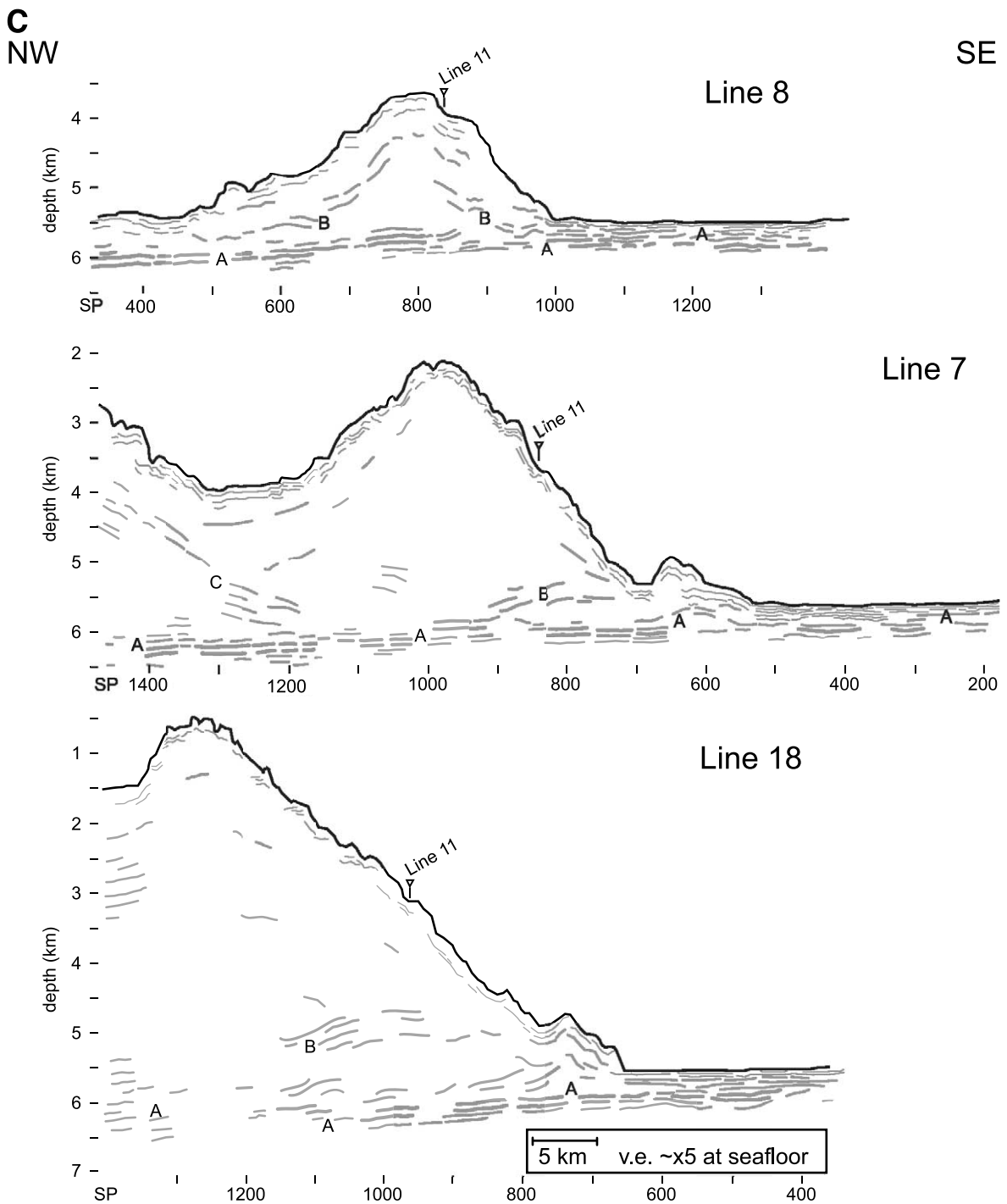


Fig. 4 (Continued). (C) Depth sections illustrating our structural interpretations. Horizon A is interpreted as a layer of sediments extending beneath the volcanic edifice. The buried flank of Hilo Ridge is interpreted to extend beneath Puna Valley to underlie Puna Ridge. Puna Valley appears to be filled primarily with volcanoclastic debris. Discontinuous, slope parallel reflections along the flanks of Puna Ridge may define extrusive flows or debris layers. Wide, reflection-poor region along the axis of the Puna Ridge is interpreted to represent a zone of steeply dipping intrusive dikes.

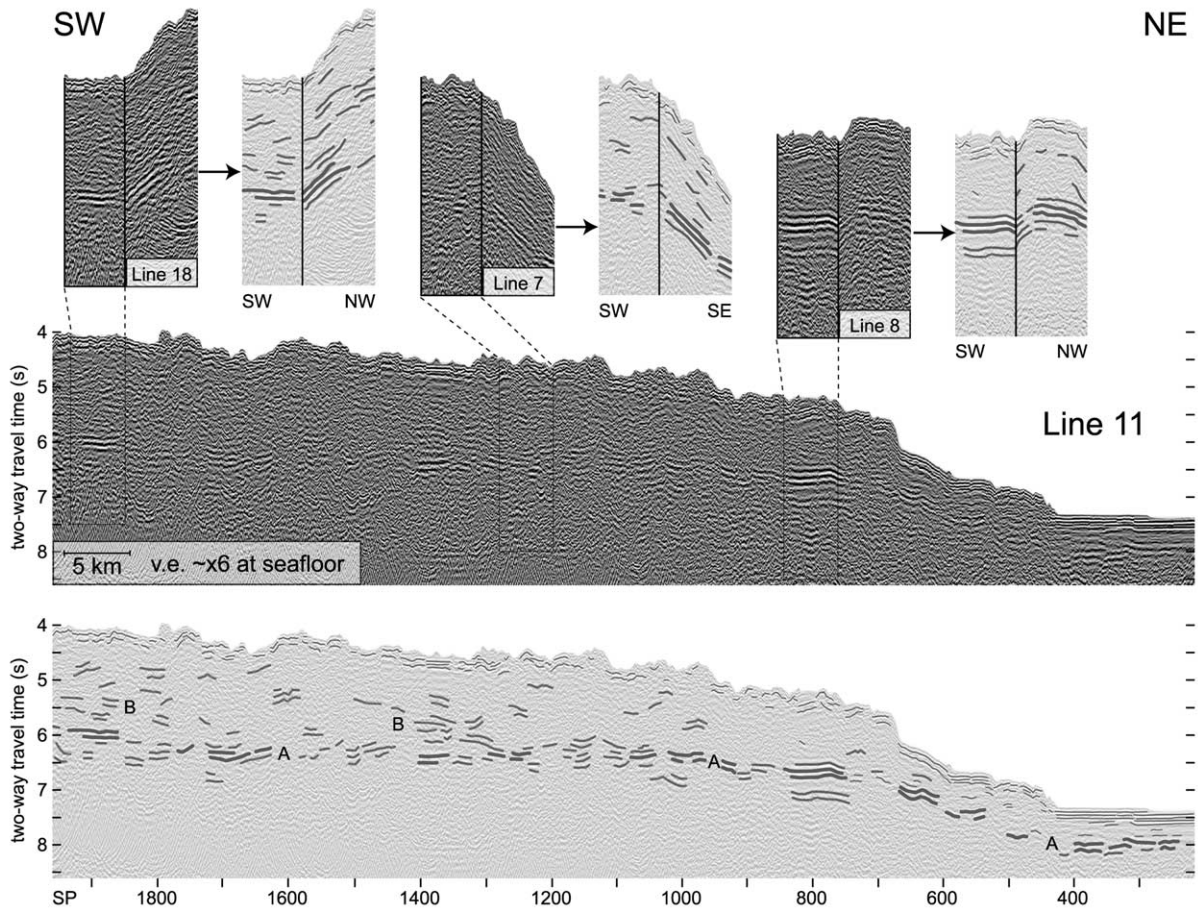


Fig. 5. Ridge parallel seismic reflection Line 11. Location is shown in Fig. 1. SP=shot point number. Note the continuous band of reflections on uninterpreted section (middle). Interpretation (bottom) shows the distribution of major reflections within the volcanic edifice as well as the location of horizon A reflections (A) and shallower reflections (B). Insets (at top) show correlations between intersecting reflection profiles in Fig. 4 and Line 11.

events of horizon A. On the depth sections (Fig. 4C), internal reflections generally dip away from the rift axis, and are concentrated along the rift flanks, particularly on Line 8 near the distal end of the ridge (e.g., Fig. 4C, SP 800–1000). In contrast, the seismic character of the zone immediately below the rift axis is typically reflection-poor, particularly on the up-rift Lines 7 (Fig. 4C, SP 850–1000) and 18 (Fig. 4C, SP 1200–1300). On these two lines, several reflections, labeled B, also rise from horizon A beneath the edifice, trending toward, but not reaching, the seafloor to the south (Fig. 4B,C).

Beneath the seaward Hawaiian Moat and the

flat seafloor of Puna Valley, sequences of sub-parallel reflections occur. The moat to the southeast exhibits a thick package of high-frequency, horizontal reflections above the continuation of horizon A (e.g., Fig. 4, Line 7, SP 200–500). To the northwest of the rift axis, reflection dips are more variable. Beneath the NW flank of Puna Ridge, reflectors generally dip to the northwest (e.g., Fig. 4C, Line 7, SP 1000–1200), but this pattern does not continue into Puna Valley. Instead, continuous, sub-horizontal reflections define the shallow valley floor (Fig. 4C, Line 7, SP 1200–1300, 4 km; Line 8, SP 350–500, 5.5–6 km). On Line 7, they are underlain by a set of southeast dipping reflec-

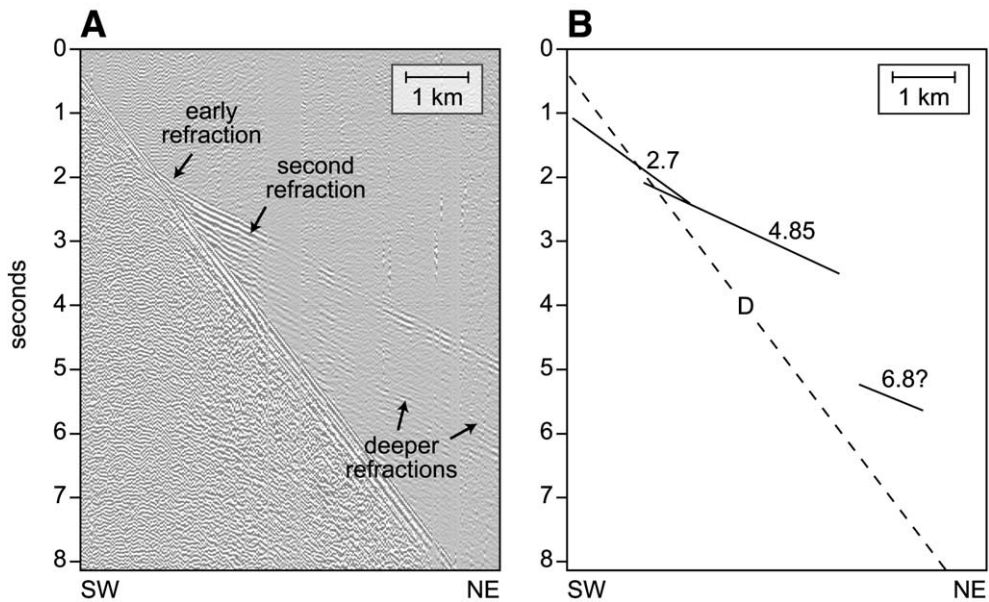


Fig. 6. Sonobuoy seismic refraction record over the shallow crest of Puna Ridge. Dashed line labeled D is the direct arrival. The first arrival has an interval velocity of 2.7 km/s and a layer thickness of ~ 850 m. The second, stronger arrival has an interval velocity of 4.85 km/s. The deepest arrivals have apparent velocities of 5–6 km/s and a loosely constrained interval velocity of 6.8 km/s.

tions, labeled C, which contrasts with the predominantly slope parallel trends within Puna Ridge (Fig. 4, SP 1200–1400, 5.5–4 km). The C reflections extend into the SE flank of Hilo Ridge, where their trend is generally parallel to the slope of the seafloor.

Line 11 (Fig. 5) is a longitudinal profile crossing the SE flank of Puna ridge that intersects the three transverse lines in Fig. 4. Horizon A is laterally continuous across the length of the ridge, and extends to the southwest beneath the submarine flank below Kilauea's subaerial edifice (Morgan et al., 2000; Hills et al., 2002). On this line, horizon A locally resolves into two parallel sets of reflections, separated by a semi-transparent zone ~ 500 ms thick (Fig. 5, SP 800, 6.7–7.2 s). This pattern of horizon A reflections is also noted seaward of the distal Puna Ridge (Fig. 5, SP 400, 7.5–8.0 s), indicating that it defines a primary feature within the moat stratigraphy. Irregular, discontinuous reflections also cut through the Puna Ridge flank above horizon A. Several of these features correlate well with the B reflections, and

other internal reflections noted on the transverse lines (Fig. 5, insets), confirming that they represent reflective discontinuities within the volcanic edifice.

4.2. Seismic refraction data

Measurements of V_p within Puna Ridge are also derived from a sonobuoy record (Fig. 6) collected over the shallow submarine axis of the ridge coincident with Line 19 (Fig. 1). These allow us to check the velocity model developed for depth conversions of the reflection lines, and reveal the distribution of velocity layers in depth within the ridge. The earliest refracted arrivals give evidence of at least two layers along the crest of Puna Ridge. The first layer, from 0 to 850 m below seafloor (mbsf), has a velocity of ~ 2.7 km/s. A second, stronger refracted arrival yields a layer velocity of 4.85 km/s located ~ 850 mbsf. Refracted arrivals on far offset channels of reflection profiles crossing the upper axis of Puna Ridge (Lines 18 and 19) also indicate velocities

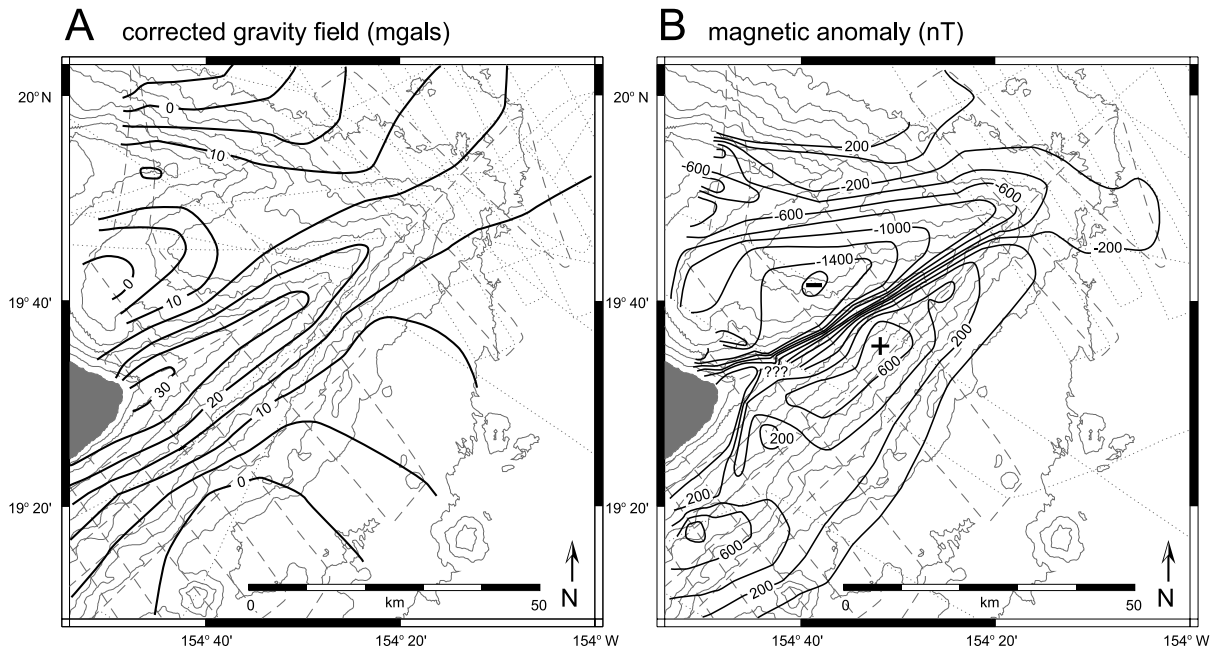


Fig. 7. Corrected gravity (A) and magnetic anomaly (B) maps of the Puna Ridge region. The +/- label indicates the axis of a large magnetic dipole formed over upper Puna Ridge. Dashed lines represent data collected during this study. Dotted lines represent data from earlier studies. Contour intervals are 5 mGal and 100 nT. Underlying bathymetry contour interval is 500 m.

of 2.7–3.7 km/s within ~ 0.5 km of the surface. Deeper refractions, or second arrivals, have apparent velocities of ~ 6.8 km/s (Fig. 6), supporting the identification of a high-velocity region near the ridge axis. Regrettably, reversed refraction profiles are not available to verify the velocity values. However, our velocities and layer thicknesses are corroborated by previous studies over the lower on-land ERZ close to the Puna Ridge (Hill, 1969; Broyles et al., 1979), and also yield similar uncertainties of ± 0.25 km/s and ± 200 m.

4.3. Gravity and magnetic data

Gravity and magnetic measurements collected along the survey track lines also show considerable anomalies adjacent to the submarine axis of the ERZ. We generated maps of the corrected gravity field (Fig. 7A) and the magnetic anomaly (Fig. 7B) from the data collected during our survey, combined with measurements made during GLORIA surveys of the area (e.g., Holcomb et

al., 1988), and data presented by Lonsdale (1989). Although the data sets differ in detail due to the spatial arrangement of ship track lines, each reveals the same general distribution of anomalies, allowing us to combine and contour the complete data sets.

A terrain-corrected gravity field was determined by modeling the predicted 3D gravity field for the submarine edifice, and subtracting this from the shipboard free air gravity measurements (Fig. 7A). Edifice densities were set to 2600 kg/m^3 , consistent with values chosen for Kilauea's submarine flanks for 3D modeling of the density structure of the entire island of Hawai'i (Kauahikaua et al., 2000). The resulting map reveals an elongate gravity high roughly paralleling Puna Ridge, indicating the existence of a body at depth beneath the submarine ERZ, with a density $> 2600 \text{ kg/m}^3$. The axis of the gravity high is offset ~ 1 km to the southeast of the topographic axis of Puna Ridge along the upper two-thirds of the length of the submarine rift zone (Fig. 7A). A similar offset gravity high was also noted over the near-

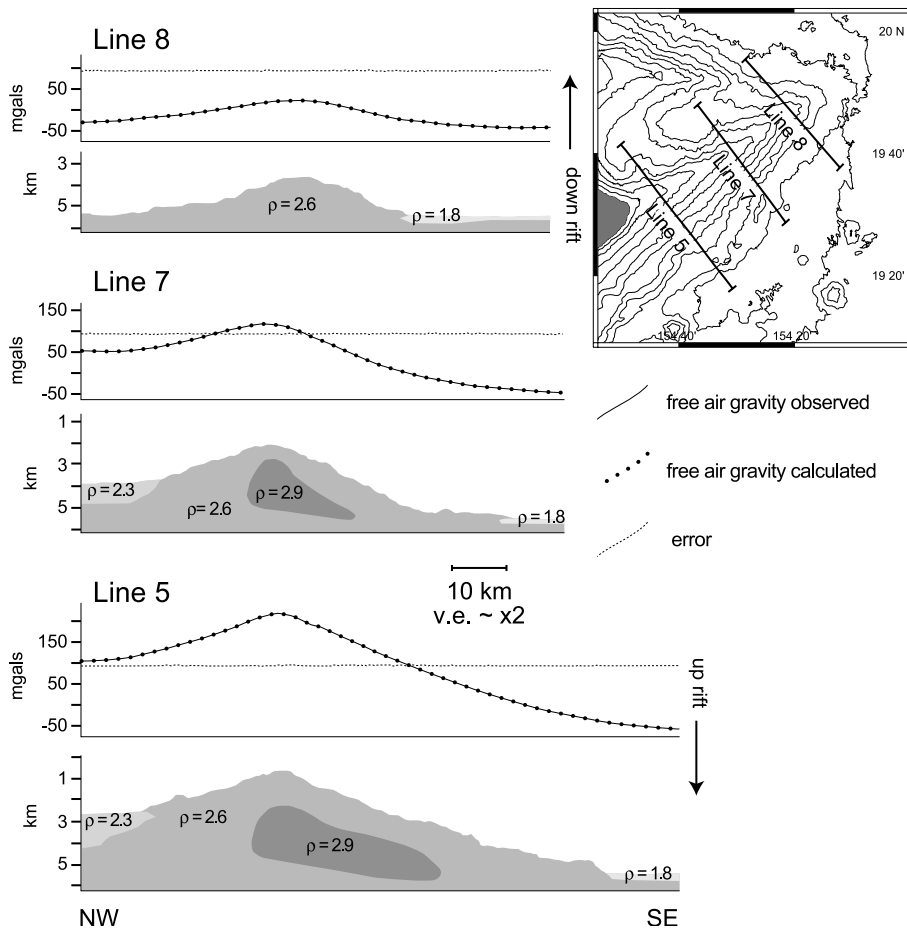


Fig. 8. Selected gravity profiles across Puna Ridge. Shown with each profile is a density model that fits the observed data and a plot of the difference between calculated and observed (error). Note that the high density ($\rho=2.9$) anomaly is offset to the south-east of the topographic axis of the ridge on the two up-rift profiles.

shore rift axis by [Kauahikaua et al. \(2000\)](#), who interpreted rift zone anomalies to result from high-density intrusive complexes. We note that the intensity of the gravity anomaly decreases significantly down-rift ([Fig. 7A](#)). Anomalously low gravity values occur between Hilo and Puna Ridges, suggesting that this area is composed of lower-density material than the surrounding volcanic ridges.

Magnetic field measurements collected over Puna Ridge reveal an elongate, normally polarized anomaly that parallels the axis of the ridge ([Fig. 7B](#)), similar to the results of [Malahoff and McCoy \(1967\)](#). The anomaly forms a closed dipole, centered along the upper portion of the sub-

marine rift zone, coincident with the high gravity anomaly. As with the gravity signal, the strength of the magnetic anomaly decreases from the dipoles towards the distal end of the rift zone ([Fig. 7B](#)), suggesting that the anomalous body decreases in volume towards the distal termination of the rift zone.

To further define the depth and dimensions of the rift zone anomaly, we modeled density variations along Puna Ridge in 2D, attempting to fit the gravity observations along ridge crossing profiles ([Fig. 8](#)). We chose densities based on previous gravity studies and rock density measurements (e.g., [Nafe and Drake, 1957](#); [Strange et al., 1965](#); [Watts and ten Brink, 1989](#); [Kauahikaua](#)

et al., 2000; Moore, 2001). Consistent with the terrain correction applied above, the volcanic edifice was assigned a density of 2600 kg/m^3 . Reasonable densities for the inferred intrusive complex range from 2900 kg/m^3 for dense intrusive dikes, to 3300 kg/m^3 for olivine cumulates (e.g., Kauahikaua et al., 2000). Lacking direct evidence for a layered complex, we assigned the intrusive body the lower density of 2900 kg/m^3 . To match the observed and calculated gravity measurements, it was also necessary to introduce a region of relatively low density (2300 kg/m^3) located between Hilo Ridge and Puna Ridge (Fig. 8). Finally, a layer of pelagic and volcanoclastic sediments ponded within the abyssal Hawaiian Moat was assigned a density of 1800 kg/m^3 . More poorly constrained density values (i.e., for materials within Puna Valley and Hawaiian Moat) were refined iteratively by minimizing the error function along the gravity profiles.

It is possible to obtain a good fit to the shipboard gravity profiles with a variety of density models, using a range of density contrasts and layer geometries; our solutions (Fig. 8), therefore, are non-unique. However, we sought to pick a simple, geologically reasonable geometry for the density anomalies along the profiles, constrained by the offset peak of the high-density anomaly and the base of the volcanic edifice (Fig. 4C). On Lines 5 and 7, we modeled a high-density body, offset and elongated to the southeast of the topographic axis of Puna Ridge and lying $\sim 1.5\text{--}3 \text{ km}$ below the crest (Fig. 8). The anomaly is asymmetric in cross-section, with the NW surface dipping more steeply than the SE surface. Line 8, in contrast, required no high-density anomaly to fit the observed gravity measurements (Fig. 8). The modeled width of the high-density intrusive body decreases rapidly down-rift, from $\sim 35 \text{ km}$ at Line 5, to $\sim 20 \text{ km}$ at Line 7, and eventually becomes undetectable by Line 8. The modeled depths would tend to increase, and the widths would decrease, if the higher density of 3300 kg/m^3 was assumed for the body.

4.4. Data interpretation

The several data sets presented here provide

constraints on the internal structure of Puna Ridge, and we seek a geologic model that can explain all of the observed characteristics. Key among these are the continuous reflections defining horizon A that underlie the entire Puna Ridge, and the high-velocity, high-density body that lies beneath and to the southeast of the upper rift axis.

As noted above, the occurrence of horizon A across the entire study area and the progressive increase in travel time beneath the volcanic edifice indicate that this feature lies at or near the top of pre-existing oceanic crust upon which the volcano grew (e.g., Watts et al., 1985; Morgan et al., 2000; Leslie et al., 2002). The high amplitude of horizon A indicates a significant impedance contrast at depth, denoting a sharp change in velocity or density across this interface. One explanation is that the reflections arise from sediment layers lying on top of the Cretaceous age oceanic crust. Up to 200 m of pelagic sediment have been documented in this region (Ewing et al., 1968; Houtz and Ludwig, 1979; Waggoner, 1993), and significant accumulations of volcanoclastic debris may have derived from mass wasting of Hawaiian volcano flanks (e.g., Moore and Chadwick, 1995; Leslie et al., 2002). In support of the sediment origin of these reflections is the similarity in reflection character of horizon A beneath and seaward of Puna Ridge, noted on Line 11 (Fig. 5). The transparent unit bounded by grouped reflections resembles the pelagic layer sandwiched between the oceanic crust and overlying turbidites and landslide debris, noted within the Hawaiian Moat by Leslie et al. (2002). These sediments were subsequently buried beneath the growing Puna Ridge.

An alternative interpretation for the strong-amplitude horizon A is that it represents a highly dilated plane beneath the volcanic ridge, perhaps indicative of high pore pressures trapped within a thin sediment layer (e.g., Iverson, 1995). This may denote a fault plane beneath the edifice (e.g., Denlinger and Okubo, 1995), also interpreted to the southeast from evidence for frontal deformation (Morgan et al., 2000; Hills et al., 2002). We would expect such a layer, however, to exhibit a negative impedance contrast with a resulting neg-

ative polarity reflection, but the observed reflection is positive (e.g., Fig. 4A). A third possibility, but more difficult to confirm, is that the reflective regions of horizon A are produced by thin sills or sheet flows beneath the ridge, similar to those that have been observed on the seafloor adjacent to the tip of Puna Ridge (Holcomb et al., 1988). However, the impedance contrast between sheet flows and bounding pillow basalts likely is not sufficient to generate such high-amplitude reflections.

The evidence for an unusually high-density, high-velocity body within Puna Ridge signifies the presence of a core of intrusive material, such as dikes or cumulates, as has been described in previous studies along the submarine ERZ (Malahoff and McCoy, 1967; Hill and Zucca, 1987). The high-apparent-velocity (6.8 km/s) refractions are interpreted as arrivals traveling through the submarine extension of the ERZ intrusive dike complex. The shallow 2.7 km/s layer is interpreted as a mantle of submarine extrusive basalt that overlies a deeper intrusive core with velocities ~ 6.8 km/s. The intermediate 4.85 km/s layer is assumed to represent a zone of mixed intrusive and extrusive rocks.

The lack of coherent reflections beneath the rift axis is also consistent with the presence of highly irregular intrusive materials, composed in part of sub-vertical dikes. Our seismic velocity models offer little constraint on the depth of the intrusive body, however, gravity modeling implies that it is relatively shallow beneath the rift axis; the top lies within 1.5–3 km below the rift axis (Fig. 8). Dikes are thought to propagate over a similar depth range (2–4 km) along the upper ERZ, based on earthquake sequences along the upper ERZ (e.g., Klein et al., 1987). The modeled anomalies on Lines 5 and 7 are restricted to the SE flank, and maintain nearly constant depths below the flank surface (Fig. 8). The broad gravity anomalies detected on Lines 5 and 7 may also have a contribution from higher-density (3300 kg/m^3) cumulates, that may concentrate below the zone of active dike propagation (Hill and Zucca, 1987; Okubo et al., 1997; Kauahikaua et al., 2000), although we have no direct evidence to support this interpretation.

The flanks of Puna Ridge are slightly more reflective than the core (e.g., Figs. 4 and 5). This suggests that the flanks have more internal layering, possibly associated with extrusive volcanism and formation of discrete lava flows and terraces. Alternatively, some of these reflections may define structural discontinuities, or incipient faults, such as the northwest dipping B reflections that rise from horizon A, preferentially beneath the SE flank (Fig. 4C, Lines 7 and 18). Similar features have been recognized beneath the volcanic flanks to the southwest, where they offset layered strata and uplift the midslope bench, and are interpreted to accommodate outward displacement of the volcanic flanks (Morgan et al., 2000; Hills et al., 2002). Below the north flank of Puna Ridge, southeast dipping reflections C extend beneath Puna Valley, and continue parallel to the slopes of Hilo Ridge, suggesting that they define the paleoslope of the older submarine ridge (Fig. 4C, Line 7). This reflection geometry denotes the overlap of the northern flank of Puna Ridge (dipping to the northwest) upon the pre-existing Hilo Ridge (dipping to the southeast). Similar overlapping relationships between Puna Ridge and the old ERZ of Mauna Loa (Holcomb et al., 2000) are possible, but cannot be confirmed here.

Low modeled densities within Puna Valley (Fig. 8), and sequences of sub-horizontal reflections within the valley, suggest the presence of unconsolidated sediments in this region. Based upon their seismic character (Fig. 4), proximity to interpreted slide scars on the northern Puna Ridge (Moore and Chadwick, 1995), and the enclosed setting between Hilo and Puna Ridges (Fig. 3), we interpret the material filling the shallow Puna Valley to be volcanoclastic debris derived from mass wasting of the surrounding submarine and subaerial volcano slopes (Moore and Chadwick, 1995; Leslie et al., 2002). The sub-horizontal reflections observed within this region are consistent with a sedimentary origin, and suggest onlap of these sediments onto the adjacent ridges. Similar low-density material must also lie within the Hawaiian Moat to the southeast, although the lower thickness of this unit produces a less pronounced anomaly.

5. Discussion

5.1. Puna Ridge substructure

One of the most striking results of this study is the recognition of continuous sub-volcanic reflections defining horizon A, extending beneath Puna Ridge and across the entire study area (Fig. 4). The high impedance contrast indicated by their high amplitude, and the pairing of reflectors observed on Line 11 (Fig. 5), support the interpretation that horizon A defines a thick package of sediments sandwiched between the volcanic edifice and the oceanic crust. Variations in amplitude and thickness of the reflections from this sediment layer imply that sediment distribution on the seafloor was uneven prior to burial beneath the volcanic edifice. Indeed, this is supported by previous studies (Leslie et al., 2002) that showed sediment thickness to vary between 300 m and 1 km directly adjacent to the active flanks of Kilauea and Loihi. The majority of this sediment is probably volcanoclastic in nature, probably derived from landslides and small-scale mass wasting, since the underlying pelagic sediment in this region is typically 80–100 m thick (Winterer, 1989; Leslie et al., 2002). Local variations in sediment thickness occur because of variations in sediment dispersal patterns, proximity to areas of slope failure, and pre-existing seafloor topography (e.g., Cretaceous age seamounts). Similar thicknesses of low-velocity sediments have also been invoked to explain velocity contrasts indicated by travel time differences between P- and S-wave arrivals beneath Mauna Loa (Thurber et al., 1989), suggesting that sediments define a ubiquitous substrate beneath Hawaiian volcanoes.

The continuous layer of sediment reflections beneath the axis of the rift zone supports the notion that Hawaiian rift zones grow axially across the seafloor and are rootless features fed by dike intrusions down the rift axis (Fiske and Jackson, 1972; Lonsdale, 1989). Thick sediment accumulations beneath the growing edifice may also provide a weak, and possibly overpressured, décollement surface beneath the volcano that can accommodate lateral displacements of the flanks (e.g., Nakamura, 1980; Denlinger and Okubo,

1995; Iverson, 1995). Reflector divergence (i.e., reflections B from horizon A) beneath the upper submarine ridge on Lines 7 and 18 (Fig. 4) suggests the presence of thrust faults along which the flank has displaced.

5.2. Rift zone intrusive complex

High V_p , gravity and magnetic anomalies, and the absence of coherent reflections within the seismic reflection record beneath the axis of the Puna Ridge, all point to the existence of an interior rift zone core composed of high-density intrusive rocks, embedded within and mantled by extrusive volcanic products. By analogy with exposed rift complexes (e.g., Fornari, 1987; Walker, 1987), we interpret this zone to consist of intersecting vertical and sub-vertical dikes that cut through the country rock, distributed with increasing intensity with depth. The dikes are a fundamental component of rift zone eruptions, and propagate laterally along the rift axis from the summit or local magma chambers (Fiske and Jackson, 1972; Klein et al., 1987; Lonsdale, 1989).

Additional intrusive components, such as dense cumulates that settled from magma reservoirs below the dike zone (e.g., Hill and Zucca, 1987; Okubo et al., 1997), are possible, but cannot be fully resolved with our data. Our estimated width of the dense rift core beneath the upper submarine Puna Ridge of 20–35 km, however, is high compared to previous estimates of an 11 km wide zone responsible for the magnetic anomaly over Puna Ridge (Malahoff and McCoy, 1967), and 12–17 km (Broyles et al., 1979; Kauahikaua et al., 2000) and 20 km (Furumoto, 1978) wide core over the subaerial lower ERZ. The greater offshore width in our models may result from the low density of 2900 kg/m³ that we assumed for the intrusive core. If higher-density cumulates are present in this region (e.g., Kauahikaua et al., 2000), the modeled intrusive complex will be reduced in size.

The geometry of the dike complex interpreted from the gravity and velocity modeling is a broad, asymmetric wedge, similar to that predicted by Hill and Zucca (1987) for the subaerial ERZ of Kilauea (Fig. 2). Unlike the subaerial ERZ, how-

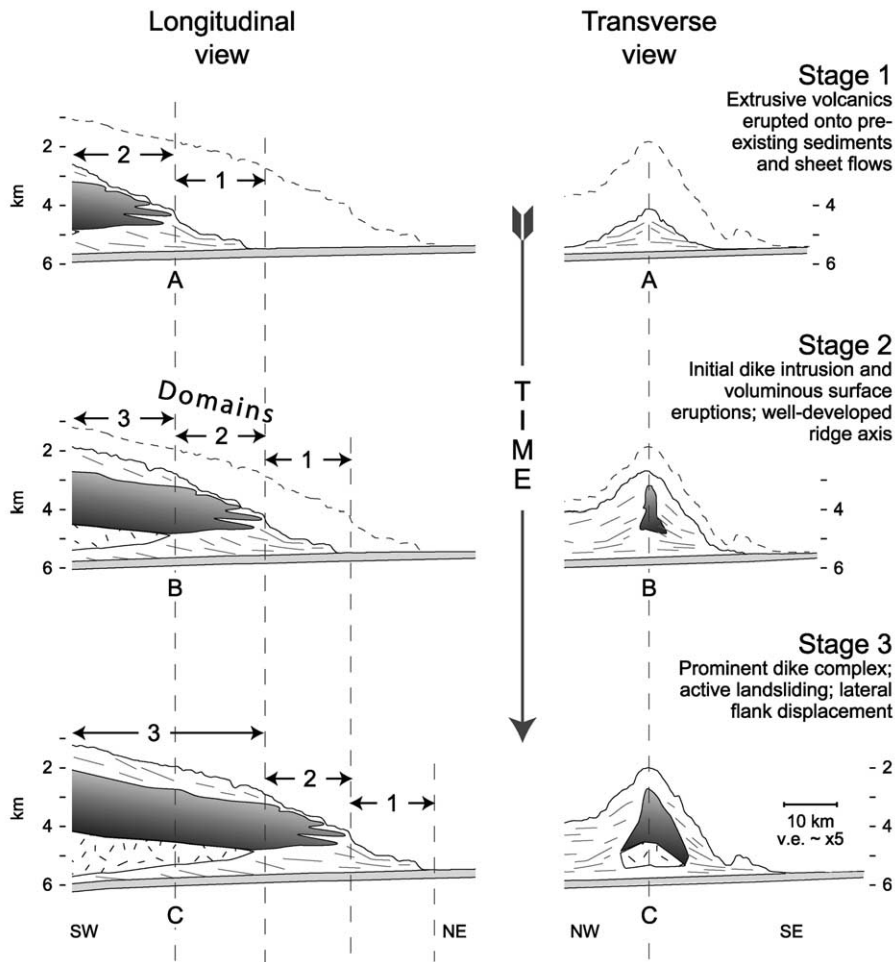


Fig. 9. Proposed model for the evolution of a rift zone built adjacent to a mature volcanic flank. Three spatial domains of the rift zone (1, 2 and 3) are defined by variations in axial slope and the presence of a high-velocity, high-density intrusive rift zone core, and propagate down-rift as the rift zone lengthens (longitudinal cross-sections). Each domain passes through distinct stages of rift zone evolution, denoted in the transverse cross-sections. The rift zone initiates during Stage 1 by accumulation of extrusive products erupted from up-rift that fill the deepest part of the nearby flexural moat. Stage 2 occurs when the rift zone reaches a height that favors dike intrusion, allowing for voluminous surface eruptions that build a well-defined axial slope $\sim 6^\circ$. The axial slope decreases to $\sim 3^\circ$ and the width of the intrusive dike zone grows rapidly during Stage 3, as dike intrusion is favored over eruption, and is accommodated by surficial landsliding and lateral displacement of the unbuttressed ridge flank. Cumulates may collect beneath the rift axis, easing rift zone spreading. Dashed line indicates the final ridge profile.

ever, where the high-density anomaly is offset to the northwest of the active rift zone (Kinoshita et al., 1963; Swanson et al., 1976; Kauahikaua et al., 2000), the intrusive core is offset to the SE side of the topographic rift axis along the upper submarine ERZ. Furthermore, we interpret a steeply dipping upper surface on the NW side of

the complex, again, in contrast with that modeled for the subaerial ERZ (Fig. 2). At first glance, our results would imply the reverse sense of rift axis migration – to the northwest, rather than to the southeast proposed for the on-land rift zone (Swanson et al., 1976; Hill and Zucca, 1987). This may be a response to landslide events along

the northern submarine flank of the rift zone, as suggested by the embayed north flank and accumulated debris within Puna Valley. However, NW migration is difficult to reconcile with the buttressing Hilo Ridge to the north. Instead, we propose that dikes intruded preferentially on the upslope side of the complex, pushing older dikes and flank to the southeast, thereby widening and displacing the intrusive complex.

Other lines of evidence also support the mobility of the south flank of Puna Ridge. The great intrusive volume of the rift complex must have been accommodated by outward displacement of the flanks, and the presence of the pre-existing Hilo Ridge to the north would favor southward displacement. Moreover, the width of Puna Ridge increases significantly between Lines 8 and 7 (Fig. 1), coincident with the increasing gravity anomaly along the axis (Figs. 7 and 8). The greater width of the near-shore ridge results from several low terraces near the base of the SE slope. Previously interpreted as slump blocks derived from the upper flanks (Clague et al., 1994), these terraces resemble the higher bench found to the southwest below the subaerial edifice of Kilauea. In that location, the frontal bench has been interpreted to arise from overthrusting at the toe of the mobile south flank (Denlinger and Okubo, 1995; Borgia and Treves, 1992; Morgan et al., 2000); Puna Ridge's low terraces may have been similarly uplifted as the ridge flank slid into surrounding sediments (Hills et al., 2002). Such terraces are absent along the base of the NW Puna Ridge, consistent with asymmetric spreading of the ridge.

5.3. Rift zone evolution

To evaluate variations in internal structure of Puna Ridge and their relationships to geomorphology, we subdivide the submarine ERZ into three domains (Fig. 9), similar to those outlined by Vogt and Smoot (1984) in their study of the flank rift zone bathymetry of North Pacific guyots. From the distal tip of the ERZ to the submarine–subaerial transition, these domains are defined by changes in rift zone morphology, including axial slope angle, and by internal rift

structure. We build upon the three regimes introduced by Vogt and Smoot (1984) and attempt to reconcile our observations with existing models for rift zone growth and propagation. We propose that these spatial domains also correspond to growth stages of Puna Ridge, and are applicable to the evolution of submarine rift zones in a wide variety of settings.

Domain 1 is characterized by the presence of primarily extrusive volcanic materials, and is currently recognized at the extreme distal 10–15 km of Puna Ridge at a depth of ~ 4500 – 5500 m (Fig. 9). During this earliest Stage 1 of rift zone development, extensive sheet flows are erupted near the tip of the rift zone, and flow outward to cover the abyssal seafloor (Holcomb et al., 1988), intermingling with mass wasting debris from failure of nearby volcanic slopes (Fig. 9, cross-section A). The topographic axis of the rift zone at this stage is ill-defined, either non-existent, or perhaps bifurcating at its termination (Lonsdale, 1989). Gravity and magnetic profiles indicate that a high-density intrusive body is absent at this stage of rift zone growth, perhaps because the edifice has not reached a height at which confining pressures are great enough to trap dikes traveling from further up-rift (Vogt and Smoot, 1984; Dieterich, 1988; Fialko and Rubin, 1999).

Domain 2 is defined by the first occurrence of dikes within the rift zone, steeper flank slopes, and the appearance of a well-defined topographic axis with a slope of $\sim 6^\circ$ (Fig. 9). Currently, this domain occurs from ~ 15 to 30 km from the end of the rift zone at water depths of 2800–4500 m. Seismic reflection profiles across this region show a collection of poorly continuous reflections dipping away from the topographic axis (Fig. 4). Gravity and magnetic anomalies become apparent within this domain, indicating an increasing number of high-density dikes beneath the axis of the rift zone. Stage 2 of rift zone development (Fig. 9, cross-section B), therefore, is marked by the initial intrusion of dikes at shallow depths along a zone of neutral buoyancy (e.g., Ryan, 1988; Fialko and Rubin, 1999). High axial slopes, a peak in differential magmatic pressure, and low horizontal trapping stresses may favor surface eruption following dike propagation, rather than magma stor-

age during Stage 2 (e.g., Dieterich, 1988; Fialko and Rubin, 1999). High-volume, enduring, rift axis eruptions across Domain 2 (e.g., Parfitt et al., 2002) would lead to rapid vertical growth of the rift zone, and progressive shallowing of the longitudinal slope to a ‘critical’ value marking the transition to Domain 3 (Lonsdale, 1989; Fialko and Rubin, 1999).

Domain 3 occurs from ~ 30 km from the distal end of the rift zone to the submarine–subaerial transition, over the depth range of 2800–0 m (Fig. 9). This domain is typified by a gentler axial slope of 3° , and strong velocity, gravity, and magnetic anomalies along the axis of the rift zone, indicative of a well-developed intrusive core. During Stage 3 (Fig. 9, cross-section C), short-lived magma reservoirs below the axial dike zone may concentrate dense cumulates near the base of the rift zone (Fig. 9), possibly easing seaward displacement of the SE flank (e.g., Clague and Deningler, 1994), and enabling further dike intrusion. The reduced rate of surface eruption leads to shallowing of the longitudinal slope of the rift axis; seaward displacement causes uplift of terraces along the distal flanks (e.g., Hills et al., 2002). Large landslide amphitheatres recognized along the north flank of Puna Ridge probably also develop during Stage 3, and may play an important role in the onset of rapid rift zone extension and flank spreading (e.g., Morgan et al., 2003).

Based on our 3D array of seismic lines over Puna Ridge, we propose that Kilauea’s ERZ evolved in a largely steady-state manner. The spatial domains shown in Fig. 9 propagate along the rift axis, as each region passes through sequential stages of rift zone development. As shown in Fig. 9, the ridge grows upward as it lengthens, maintaining a consistent profile that migrates seaward with time. The propagating ridge tip laps down upon the abyssal seafloor, and is subsequently intruded by dikes traveling along the rift zone at shallow depths (Fig. 9) along a zone of neutral buoyancy (e.g., Ryan, 1988; Fialko and Rubin, 1999); these locally feed surface eruptions, preferentially along the distal reaches of the rift zone, where the topographic slopes are highest. By this model, the ERZ of Kilauea will continue to elongate as the volcano grows, building outward and

spreading to the southeast with further dike intrusion. The growth stages described here may represent the evolution of volcanic rift zones in many submarine settings, although local variations in volcanic edifice configuration or seafloor topography may influence the final rift zone structure and geometry.

6. Conclusions

New seismic reflection and refraction, gravity, and magnetic data across Puna Ridge, the submarine extension of Kilauea Volcano’s ERZ, help to resolve the subsurface structure of the active rift zone. A pronounced set of reflections, corresponding to the top of the pre-existing oceanic crust and overlying pelagic and volcanoclastic sediments, underlies the entire ridge. The continuity of these reflectors indicates that the oceanic crust is unbroken, and the rift zone grew by down-rift migration of magma from the summit magma chamber, rather than by vertical emplacement through the seafloor. Reflections within the flanks of Puna Ridge generally dip outward, and are thought to reflect primary layering of extrusive materials. Several deeper reflections diverge from the oceanic crust reflector and dip toward the rift. Along the SE flank, these may represent incipient thrust faults accommodating seaward displacement of the flank; beneath the NW flank and Puna Valley, strong southeast dipping reflections appear to mark the paleoslope of Hilo Ridge, indicating growth of Puna Ridge upon the older volcanic rift zone.

An asymmetric body of high V_p , high density, and magnetic materials is indicated beneath the axis of the submarine rift zone. Gravity modeling places this anomaly at shallow depths and slightly offset to the southeast of the ridge axis. We interpret this body to define an intrusive core of dikes and cumulates, embedded within and mantled by extrusive volcanic products. The width of the dike complex is estimated at 35 km along the upper submarine rift, and decreases down-rift to become undetectable near the distal end of Puna Ridge. The SE offset of the intrusive core is best explained by the progressive intrusion of dikes and

deep cumulates at the rift axis, as the SE flank is displaced seaward. The pre-existing Hilo Ridge may have buttressed the NW flank, preventing symmetric spreading of the ridge. Low-velocity materials modeled within Puna Valley to the north of the ridge, and the Hawaiian moat to the south, are interpreted to be volcanoclastic debris shed from the nearby slopes.

Longitudinal changes in axial slope along Puna Ridge coincide with lateral changes in width of the intrusive core and dimension of Puna Ridge, and may relate to the mobility of the south flank. The morphology and substructure of the ridge allow us to define three domains corresponding to growth stages of the rift zone. Domain 1, at the distal end of the ridge, shows irregular slopes and no rift core, defining the earliest Stage 1 of Puna Ridge growth, as it laps down onto the abyssal seafloor. Domain 2 reveals higher axial slopes, a narrow intrusive core, suggesting that Stage 2 defines a phase of rapid eruption and volcanic accretion as the rift zone lengthens and grows upward. Domain 3, along the near-shore submarine ridge, is characterized by shallow axial slopes and a wide intrusive core. Widening of the ridge and formation of low terraces along the lower slopes across this domain suggest that the SE flank has been displaced outward to accommodate dike intrusion. Stage 3, therefore, marks the onset of flank mobility, possibly enabled by cumulate developed below the rift axis.

Acknowledgements

This study was supported by National Science Foundation Grant OCE-9711715. We thank the shipboard scientific party and professional crew of the *R/V Maurice Ewing*. Christian Berndt provided assistance recovering the sonobuoy data. We acknowledge the support of this research by Landmark Graphics Corporation via the Landmark University Grant Program. Thoughtful reviews by D. Smith, R. Holcomb, B. Eakins, F. Duennebie, and M. Garcia contributed significantly to the improvement of this manuscript. SOEST contribution #6270.

References

- Ando, M., 1979. The Hawai'i earthquake of November 29, 1975; low dip angle faulting due to forceful injection of magma. *J. Geophys. Res.* 84, 7616–7626.
- Armstrong, T., McAteer, J., Connolly, P., 2001. Removal of overburden velocity anomaly effects for depth conversion. *Geophys. Prospect.* 49, 79–99.
- Borgia, A., Treves, B., 1992. Volcanic plates overriding the oceanic crust: structure and dynamics of Hawaiian volcanoes. In: Parson, L.M., Murton, B.J., Browning, P. (Eds.), *Ophiolites and their Modern Oceanic Analogues*. Geological Society, London, pp. 277–299.
- Broyles, M., Suyenaga, W., Furumoto, A.S., 1979. Structure of the lower East Rift Zone of Kilauea Volcano, Hawai'i, from seismic and gravity data. *J. Volcanol. Geotherm. Res.* 5, 317–336.
- Clague, D.A., Denlinger, R.P., 1994. Role of olivine cumulates in destabilizing the flanks of Hawaiian volcanoes. *Bull. Volcanol.* 56, 425–434.
- Clague, D.A., Hon, K.A., Anderson, J.L., Chadwick, W.W., Jr., Fox, C.G., 1994. Bathymetry of Puna Ridge, Kilauea Volcano, Hawai'i. Misc. Field Studies Map, U.S. Geological Survey, MF-2237.
- Clague, D.A., Moore, J.G., Reynolds, J.R., 2000. Formation of submarine flat-topped volcanic cones in Hawai'i. *Bull. Volcanol.* 62, 214–233.
- Crosson, R.S., Endo, E.T., 1982. Focal mechanisms and locations of earthquakes in the vicinity of the 1975 Kalapana earthquake aftershock zone 1970–1979: Implications for tectonics of the south flank of Kilauea Volcano, Island of Hawai'i. *Tectonics* 1, 495–542.
- Delaney, P.T., Denlinger, R.P., 2000. Stabilization of volcanic flanks by dike intrusion. *Bull. Volcanol.* 61, 356–362.
- Delaney, P.T., Denlinger, R.P., Lisowski, M., Miklius, A., Okubo, P.G., Okamura, A.T., Sako, M.K., 1998. Volcanic spreading at Kilauea, 1976–1996. *J. Geophys. Res.* 103, 18003–18023.
- Delaney, P.T., Fiske, R.S., Miklius, A., Okamura, A.T., Sako, M.K., 1990. Deep magma body beneath the summit and rift zones of Kilauea volcano, Hawai'i. *Science* 247, 1311–1316.
- Denlinger, R.P., Okubo, P., 1995. Structure of the mobile south flank of Kilauea volcano, Hawai'i. *J. Geophys. Res.* 100, 24499–24507.
- Dieterich, J.H., 1988. Growth and persistence of Hawaiian volcanic rift zones. *J. Geophys. Res.* 93, 4258–4270.
- Ewing, J., Ewing, M., Aitken, T., Ludwig, W.J., 1968. North Pacific sediment layers measured by seismic profiling. In: Knopoff, L., Drake, C.L., Hart, P.J. (Eds.), *The Crust and Upper Mantle of the Pacific Area*. Geophys. Monogr. Ser. 12, 147–173.
- Fialko, Y.A., Rubin, A.M., 1999. What controls the along-strike slopes of volcanic rift zones? *J. Geophys. Res.* 104, 20007–20020.
- Fiske, R.S., Jackson, E.D., 1972. Orientation and growth of Hawaiian volcanic rifts: The effects of regional structure and

- gravitational stresses. *Proc. R. Soc. London Ser. A* 329, 299–326.
- Fornari, D.J., Malahoff, A., Heezen, B.C., 1978. Volcanic structure of the crest of the Puna Ridge, Hawai'i: Geophysical implications of submarine volcanic terrain. *Geol. Soc. Am. Bull.* 89, 605–616.
- Fornari, D.J., 1987. The geomorphic and structural development of Hawaiian submarine rift zones. In: Decker, R.W., Wright, T.L., Stauffer, P.H. (Eds.), *Volcanism in Hawai'i*. U.S. Geol. Surv. Prof. Pap. 1350, 125–132.
- Foster, D.J., Mosher, C.C., 1992. Suppression of multiple reflections using the Radon transform. *Geophysics* 57, 386–395.
- Furumoto, A.S., 1978. Nature of the magma conduit under the east rift zone of Kilauea volcano, Hawai'i. *International Geodynamics Conference, Magma Genesis Symposium, Tokyo*, p. 238.
- Gee, M.J.R., Masson, D.G., Watts, A.B., Mitchell, N.C., 2001. Offshore continuation of volcanic rift zones, El Hierro, Canary Islands. *J. Volcanol. Geotherm. Res.* 105, 107–119.
- Got, J.-L., Frechet, J., Klein, F.W., 1994. Deep fault plane geometry inferred from multiplet relative relocation beneath the south flank of Kilauea. *J. Geophys. Res.* 99, 15375–15386.
- Hill, D.P., 1969. Crustal structure of the Island of Hawai'i from seismic-refraction measurements. *Bull. Seismol. Soc. Am.* 59, 101–130.
- Hill, D.P., Zucca, J.J., 1987. Geophysical constraints on the structure of Kilauea and Mauna Loa volcanoes and some implications for seismomagmatic processes. In: Decker, R.W., Wright, T.L., Stauffer, P.H. (Eds.), *Volcanism in Hawai'i*. U.S. Geol. Surv. Prof. Pap. 1350, 903–917.
- Hills, D.J., Morgan, J.K., Moore, G.F., Leslie, S.C., 2002. Structural variability along the submarine south flank of Kilauea volcano, Hawai'i, from a multichannel seismic reflection survey. In: Takahashi, E., Lipman, P.W., Garcia, M.O., Naka, J., Aramaki, S. (Eds.), *Evolution of Hawaiian Volcanoes: Recent Progress in Deep Underwater Research*. AGU Monogr. 128, 105–123.
- Holcomb, R.T., Moore, J.G., Lipman, P.W., Belderson, R.H., 1988. Voluminous submarine lava flows from Hawaiian volcanoes. *Geology* 16, 400–404.
- Holcomb, R.T., Nelson, B.K., Reiners, P.W., Sawyer, N.L., 2000. Overlapping volcanoes: The origin of Hilo Ridge, Hawai'i. *Geology* 28, 547–550.
- Houtz, R.E., Ludwig, W.J., 1979. Distribution of reverberant subbottom layers in the Southwest Pacific Basin. *J. Geophys. Res.* 84, 3497–3504.
- Iverson, R.M., 1995. Can magma-injection and groundwater forces cause massive landslides on Hawaiian volcanoes? *J. Volcanol. Geotherm. Res.* 66, 295–308.
- Johnson, K.T.M., Reynolds, J.R., Vonderhaar, D., Smith, D.K., Kong, S.L., 2002. Petrological systematics of submarine basalt glasses from the Puna Ridge, Hawai'i: implications for rift zone plumbing and magmatic processes. In: Takahashi, E., Lipman, P.W., Garcia, M.O., Naka, J., Aramaki, S. (Eds.), *Evolution of Hawaiian Volcanoes: Recent Progress in Deep Underwater Research*. AGU Monogr. 128, 143–159.
- Kauhikaua, J., Hildenbrand, T., Webring, M., 2000. Deep magmatic structures of Hawaiian volcanoes, imaged by three-dimensional gravity models. *Geology* 28, 883–886.
- Kinoshita, W.T., Krivoy, H.L., Mabey, D.R., MacDonald, R.R., 1963. Gravity survey of the island of Hawai'i, Geological Survey Research 1963. U.S. Geol. Surv. Prof. Pap. 475, 114–116.
- Klein, F.W., 1981. A linear gradient crustal model for south Hawai'i. *Bull. Seismol. Soc. Am.* 71, 1503–1510.
- Klein, F.W., Koyanagi, R.Y., Nakata, J.S., Tanigawa, W.R., 1987. The seismicity of Kilauea's magma system. In: Decker, R.W., Wright, T.L., Stauffer, P.H. (Eds.), *Volcanism in Hawai'i*. U.S. Geol. Surv. Prof. Pap. 1350, 1019–1185.
- Leslie, S.C., Moore, G.F., Morgan, J.K., Hills, D.J., 2002. Seismic stratigraphy of the frontal Hawaiian Moat: implications for sedimentary processes at the leading edge of an oceanic hotspot trace. *Mar. Geol.* 184, 143–162.
- Lipman, P.W., Lockwood, J.P., Okamura, R.T., Swanson, D.A., Yamashita, K.M., 1985. Ground deformation associated with the 1975 magnitude-7.2 earthquake and resulting changes in activity of Kilauea Volcano, Hawai'i. U.S. Geol. Surv. Prof. Pap. 1276, 1–45.
- Lonsdale, P., 1989. A geomorphological reconnaissance of the submarine part of the East Rift Zone of Kilauea Volcano, Hawai'i. *Bull. Volcanol.* 51, 123–144.
- Macdonald, G.A., Abbott, A.T., Peterson, F.L., 1983. *Volcanoes in the Sea, The Geology of Hawai'i*. University of Hawai'i Press, Honolulu, HI, 517 pp.
- Malahoff, A., McCoy, F., 1967. The geologic structure of the Puna submarine ridge, Hawai'i. *J. Geophys. Res.* 72, 541–548.
- MBARI (Monterey Bay Aquarium Research Institute) Mapping Team, 2000. MBARI Hawai'i Multibeam Survey, 2-CD set. Digital Data Series 2, Moss Landing, CA.
- Moore, J.G., 1971. Bathymetry and Geology; East Cape of the Island of Hawai'i. U.S.G.S. Misc. Invest. Ser. I-0677, 1971.
- Moore, J.G., 2001. Density of basalt core from Hilo drill hole, Hawai'i. *J. Volcanol. Geotherm. Res.* 112, 221–230.
- Moore, J.G., Chadwick, W.W., Jr., 1995. Offshore geology of Mauna Loa and adjacent areas, Hawai'i. In: Rhodes, J.M., Lockwood, J.P. (Eds.), *Mauna Loa Revealed: Structure, Composition, History, and Hazards*. AGU Monogr. 92, 21–44.
- Moore, J.G., Clague, D.A., Holcomb, R.T., Lipman, P.W., Normark, W.R., Torresan, M.E., 1989. Prodigious submarine landslides on the Hawaiian Ridge. *J. Geophys. Res.* 94, 17465–17484.
- Moore, J.G., Clague, D.A., 1992. Volcano growth and evolution of the island of Hawai'i. *Geol. Soc. Am. Bull.* 104, 1471–1484.
- Moore, J.G., Fiske, R.S., 1969. Volcanic substructure inferred from dredge samples and ocean-bottom photographs, Hawai'i. *Geol. Soc. Am. Bull.* 80, 1191–1201.
- Moore, J.G., Krivoy, H.L., 1964. The 1962 flank eruption of

- Kilauea Volcano and structure of the east rift zone. *J. Geophys. Res.* 69, 2033–2045.
- Morgan, J.K., Moore, G.F., Clague, D.A., 2003. Slope failure and volcanic spreading along the submarine south flank of Kilauea volcano, HI. *J. Geophys. Res.* 108, p. EPM1-1-23.
- Morgan, J.K., Moore, G.F., Hills, D.J., Leslie, S.C., 2000. Overthrusting and sediment accretion along Kilauea's mobile south flank, Hawai'i: Evidence for volcanic spreading from marine seismic reflection data. *Geology* 28, 667–670.
- Nafe, J.E., Drake, C.L., 1957. Variation with depth in shallow and deep water marine sediments of porosity, density and the velocities of compressional and shear waves. *Geophysics* 22, 523–552.
- Nakamura, K., 1980. Why do long rift zones develop in Hawaiian volcanoes? A possible role of thick oceanic sediments. *Bull. Volcanol. Soc. Japan* 25, 255–269.
- Okubo, P.G., Benz, H.M., Chouet, B.A., 1997. Imaging the crustal magma sources beneath Mauna Loa and Kilauea volcanoes, Hawai'i. *Geology* 25, 867–870.
- Owen, S., Segall, P., Freymueller, J.T., Miklius, A., Denlinger, R.P., Arnadottir, T., Sako, M.K., Bürgmann, R., 1995. Rapid deformation of the south flank of Kilauea Volcano, Hawai'i. *Science* 267, 1328–1332.
- Owen, S., Segall, P., Lisowski, M., Miklius, A., Denlinger, R.P., Sako, M.K., 2000. Rapid deformation of Kilauea Volcano: Global positioning system measurements between 1990 and 1996. *J. Geophys. Res.* 105, 18983–18998.
- Parfitt, E.A., Gregg, T.K.P., Smith, D.K., 2002. A comparison between subaerial and submarine eruptions at Kilauea Volcano, Hawai'i: Implications for the thermal viability of lateral feeder dikes. *J. Volcanol. Geotherm. Res.* 113, 213–242.
- Rubin, A.M., Pollard, D.P., 1987. Origins of blade-like dikes in volcanic rift zones. In: Decker, R.W., Wright, T.L., Stauffer, P.H. (Eds.), *Volcanism in Hawai'i*. U.S. Geol. Surv. Prof. Pap. 1350, 1449–1470.
- Ryan, M.P., 1988. The mechanics and three-dimensional internal structure of active magmatic systems: Kilauea volcano, Hawai'i. *J. Geophys. Res.* 93, 4213–4248.
- Smith, D.K., Cann, J.R., 1999. Constructing the upper crust of the Mid-Atlantic Ridge; a reinterpretation based on the Puna Ridge, Kilauea Volcano. *J. Geophys. Res.* 104, 25379–25399.
- Smith, D.K., Kong, L.S.L., Johnson, K.T.M., Reynolds, J.R., 2002a. Volcanic morphology of the submarine Puna Ridge, Kilauea Volcano. In: Takahashi, E., Lipman, P.W., Garcia, M.O., Naka, J., Aramaki, S. (Eds.), *Evolution of Hawaiian Volcanoes: Recent Progress in Deep Underwater Research*. AGU Monogr. 128, 125–142.
- Smith, J.R., Satake, K., Suyehiro, K., 2002b. Deepwater multi-beam sonar surveys along the southeastern Hawai'i Ridge: Guide to the CD-ROM. In: Takahashi, E., Lipman, P.W., Garcia, M.O., Naka, J., Aramaki, S. (Eds.), *Evolution of Hawaiian Volcanoes: Recent Progress in Deep Underwater Research*. AGU Monogr. 128, 3–10.
- Stearns, H.T., Macdonald, G.A., 1946. Geology and groundwater resources of the Island of Hawai'i. Hawai'i Div. Hydrogr. Bull. 9, 363 pp.
- Strange, W.E., Woollard, G.P., Rose, J.C., 1965. An analysis of the gravity field over the Hawaiian Islands in terms of crustal structure. *Pac. Sci.* 19, 381–389.
- Swanson, D.A., Duffield, W.A., Fiske, R.S., 1976. Displacement of the south flank of Kilauea Volcano: The result of forceful intrusion of magma into the rift zones. *U.S. Geol. Surv. Prof. Pap.* 963, 1–39.
- Taylor, B., Moore, G.F., Leslie, S.C., 1998. Attenuation of reverberations using radon transforms: Example of R/V *Ewing* data from offshore Hawai'i. *EOS Trans. AGU* 79, 1008.
- Thurber, C.H., Gripp, A.E., 1988. Flexure and seismicity beneath the south flank of Kilauea Volcano and tectonic implications. *J. Geophys. Res.* 93, 4271–4278.
- Thurber, C.H., Li, Y., Johnson, C., 1989. Seismic detection of a low-velocity layer beneath the southeast flank of Mauna Loa, Hawai'i. *Geophys. Res. Lett.* 16, 649–652.
- Tilling, R.I., Dvorak, J.J., 1993. Anatomy of a basaltic volcano. *Nature* 363, 125–133.
- Vogt, P.R., Smoot, N.C., 1984. The Geisha Guyots: Multi-beam bathymetry and morphometric Interpretation. *J. Geophys. Res.* 89, 11085–11107.
- Waggoner, D.G., 1993. The age and alteration of Central Pacific Oceanic Crust near Hawai'i, Site 843. In: Wilkens, R., Firth, J., Bender, J. (Eds.), *Proc. ODP Sci. Results* 136, 119–132.
- Walker, G., 1987. The dike complex of Koolau Volcano, Oahu: internal structure of a Hawaiian rift zone. In: Decker, R.W., Wright, T.L., Stauffer, P.H. (Eds.), *Volcanism in Hawai'i*. U.S. Geol. Surv. Prof. Pap. 1350, 961–991.
- Watts, A.B., ten Brink, U.S., Buhl, P., Brocher, T.M., 1985. A multichannel seismic study of lithospheric flexure across the Hawaiian-Emperor seamount chain. *Nature* 315, 105–111.
- Watts, A.B., ten Brink, U.S., 1989. Crustal structure, flexure, and subsidence history of the Hawaiian Islands. *J. Geophys. Res.* 94, 10473–10500.
- Winterer, E.L. 1989. Sediment thickness map of the northeast Pacific. In: Winterer, E.L., Hussong, D.M., Decker, R.W. (Eds.), *The Hawaiian-Emperor Chain: The Eastern Pacific Ocean and Hawai'i*. Geol. Soc. Am., Boulder, CO, pp. 187–287.
- Wolfe, E.W., Garcia, M.O., Jackson, D.B., Koyanagi, R.Y., Neal, C.A., Okamura, A.T., 1987. The Pu'u O'o eruption of Kilauea Volcano, episodes 1–20, January 3, 1983, to June 8, 1984. *U.S. Geol. Surv. Prof. Pap.* 1350, 471–508.